3. Ya. B. Zel'dovich and Yu. P. Raizer, Physics of Shock Waves and High-Temperature Hydrodynamic Phenomena [in Russian], Nauka, Moscow (1966).
4. V. G. Kamenskii and V. L. Pokrovskii, "Finite-amplitude sound near a critical point," Zh. Éksp. Teor. Fiz., 56, No. 6 (1969).

SPHERICAL DETONATION WAVES IN MEDIA WITH VOLUMETRIC VISCOSITY

G. M. Lyakhov and V. N. Okhitin

UDC 624.131+532.529

Many solid and liquid media have volumetric viscosity appearing in dynamic processes associated with change of volume. Below we investigate detonation waves in a medium with volumetric viscosity given by the model [1] intended for the description of water-saturated soils, liquids with gas bubbles, and other multicomponent media. In these media the volume deformations are almost reversible and the tangential stresses are negligibly small, which makes it possible to investigate the effect of volumetric viscosity on the propagation characteristics of intense waves without the complicating effect of other factors. The differences in the diagrams of the corresponding shock (dynamic) compression and equilibrium state (static compression), and also the time required for establishing equilibrium in these media, are small. In the present work the problem of propagation of a spherical wave generated by the detonation of an explosive charge in a medium with volumetric viscosity and also for a nonviscous medium with the compressibility diagram corresponding to the equilibrium state is solved with the use of a computer. The corresponding results for plane waves were obtained in [1-3]. In the case of spherical waves in unsaturated soils it is necessary to use the Mises–Schleicher plasticity condition [4]. Models where the viscosity term is introduced in the plasticity condition [5] are also recommended for describing dynamic processes in solids.

§1. We consider waves in a water-saturated soil, i.e., a three-dimensional medium (solid particles, water, gas bubbles) described by the model of [1]. We denote by α_1, α_2, and α_3 the volume content of the gaseous, liquid, and solid components, by V_{10}, V_{20}, and V_{30} their volumes, by ρ_{10}, ρ_{20}, and ρ_{30} their densities, by c_{10}, c_{20}, and c_{30} the speed of sound in them, by ρ_0 the density of the three-dimensional medium, and by V_0 its specific volume. All the quantities pertain to the atmospheric pressure p_0, $\rho_0 = \alpha_1\rho_{10} + \alpha_2\rho_{20} + \alpha_3\rho_{30}$, $\alpha_1 + \alpha_2 + \alpha_3 = 1$.

At a pressure p these parameters are denoted by V_1, V_2, V_3, ρ_1, ρ_2, ρ_3, ρ, and V, respectively. In water with gas bubbles $\alpha_3 = 0$.

It is assumed that in the free state all the components are compressed according to the equation

$$\rho = p_0 + \frac{\rho_{i0}c_{i0}^2}{\gamma_i}\left[\left(\frac{V_{i0}}{V_i}\right)^{\gamma_i} - 1\right] \qquad (1.1)$$

(i is the number of the component) which corresponds to the Poisson adiabat for a gas and the theta equation for the liquid and solid components.

The gas in the medium occurs in the form of small-scale bubbles isolated from each other by the remaining components. Under the action of a load the liquid and solid components are compressed instantaneously, while the gaseous component gets compressed in a finite time, since its compression is caused by the displacement of the other components and by the filling of the initial volume of the bubbles by the other components. Therefore, the compression of air in the medium is given by the equation

Moscow. Translated from Zhurnal Prikladnoi Mekhaniki i Tekhnicheskoi Fiziki, No. 6, pp. 126-137, November-December, 1977. Original article submitted November 5, 1976.

 0021-8944/77/1806-0834$07.50

$$p = p_0 \frac{\rho_{10} c_{10}^2}{\gamma_1}\left[\left(\frac{V_{10}}{V_1}\right)^{\gamma_1} - 1\right] - \eta \frac{\dot{V}_1}{V_{10}}$$

instead of (1.1) (η is the coefficient of viscosity).

The equation of compression and discharge of the three-dimensional medium under these assumptions has the form

$$\dot{V}/V_0 = \varphi(p)\dot{p} - \alpha_1 \psi(p, V)/\eta, \tag{1.2}$$

where

$$\varphi(p) = \sum_{i=2}^{3} \frac{\alpha_i}{\rho_{i0} c_{i0}^2}\left[\frac{\gamma_i (p - p_0)}{\rho_{i0} c_{i0}^2} + 1\right]^{-(1+\gamma_i)/\gamma_i};$$

$$\psi(p, V) = p - p_0 \alpha_1^{\gamma_1}\left\{\frac{V}{V_0} - \sum_{i=2}^{3} \alpha_i \left[\frac{\gamma_i (p - p_0)}{\rho_{i0} c_{i0}^2} + 1\right]^{-1/\gamma_i}\right\}^{-\gamma_i}.$$

The equation of the shock (dynamic) compressibility of the medium ($\dot{V} \to \infty$, $\dot{p} \to \infty$) is

$$\frac{V_D}{V_0} = \alpha_1 + \sum_{i=2}^{3} \alpha_1 \left[\frac{\gamma_i (p - p_0)}{\rho_{i0} c_{i0}^2} + 1\right]^{-1/\gamma_i}, \quad \varphi(p) = \rho_0 \frac{dV_D}{dp}. \tag{1.3}$$

The equation of static compressibility ($\dot{V} \to 0$, $\dot{p} \to 0$) is

$$\frac{V_S}{V_0} = \sum_{i=1}^{3} \alpha_i \left[\frac{\gamma_i (p - p_0)}{\rho_{i0} c_{i0}^2} + 1\right]^{-1/\gamma_i}. \tag{1.4}$$

The static compressibility pertains to the equilibrium state when all the components are compressed to the limit corresponding to the applied pressure; the dynamic compressibility pertains to the compression of only the solid and liquid components. Equation (1.4) coincides with the equation of compressibility of the multicomponent medium described by the model proposed earlier disregarding the volumetric viscosity [6]. The problem of propagation and reflection of plane [7, 8, 1] and spherical [9] waves in accordance with this model has been solved. In [10] a model is proposed which takes account of the compressibility of the gas in another way. The relaxation of tangential stresses is taken into consideration in the model of [11].

Water-saturated soils occur abundantly in nature. The content of the gaseous component usually lies in the range $0 \leq \alpha_1 \leq 0.05$; the radius of the gas bubbles is in the range $0.001 \text{ cm} \leq r_* \leq 0.05$ cm, the content of the liquid component is in the range $0.2 \leq \alpha_2 \leq 0.5$. With respect to the granulometric composition water-saturated soils may be sandy or clay type. The volume deformations are reversible and the tangential stresses are negligibly small.

The detonation of the explosive is assumed to be instantaneous. The isentropic equation of the detonation products has the following form [1, 9, 12]:

$$p = A\rho^n + B\rho^{\gamma+1}. \tag{1.5}$$

At large and small pressures it goes over into the equations

$$p = p_n (\rho/\rho_n)^{k_n}; \tag{1.6}$$

$$p = p_0 (\rho/\rho_0)^{k_0}. \tag{1.7}$$

The pressure p_n and density ρ_n correspond to instantaneous detonation; p_0, ρ_0 correspond to the atmospheric pressure. The quantities A, B, n, and γ are determined from the conditions that the curves (1.5), (1.6) have a common point p_n, ρ_n and a common tangent at this point, and curves (1.5), (1.7) have a common tangent for $\rho \to 0$. During the expansion from p_n, ρ_n the detonation products do work equal to the explosion conversion heat Q.

These conditions combined with (1.5) yield a closed system of equations for determining A, B, n, and γ:

$$k_n = n + B\rho_n^{\gamma+1}(\gamma + 1 - n)\, p_n^{-1}, \quad \gamma = k_0 - 1,$$

$$Q = \frac{p_n}{\rho_n (n-1)} + \frac{B\rho_n^{\gamma}}{\gamma (n-1)}(n - \gamma - 1).$$

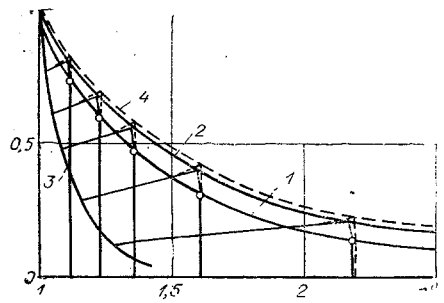

Fig. 1

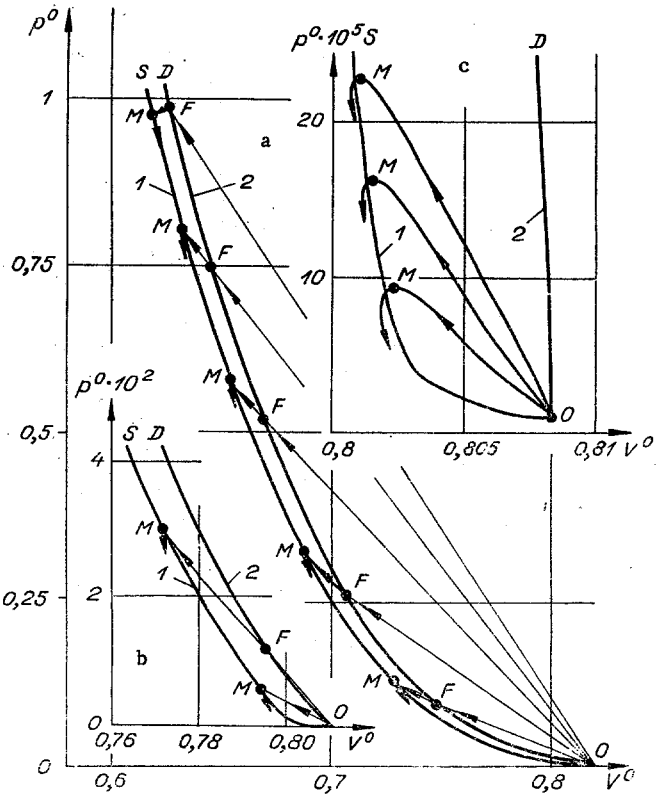

Fig. 2

In Lagrange variables the basic equations of motion have the following form (r is the spatial coordinate, t is time):

$$\frac{\partial V}{\partial t} + \frac{1}{\rho_0}\left(\frac{R}{r}\right)^{\nu}\frac{\partial u}{\partial r} = \frac{\nu u V}{R}, \quad \frac{\partial u}{\partial t} + \frac{1}{\rho_0}\left(\frac{R}{r}\right)^{\nu}\frac{\partial p}{\partial r} = 0, \tag{1.8}$$

where R is the Eulerian coordinate; $\nu = 2$; $\partial R/\partial t = u$.

The solution of the problem reduces to the integration of system (1.8) closed by Eq. (1.2). The boundary conditions are as follows:

At the boundary of the gas chamber, i.e., at $r = r_0$, due to the assumed scheme of instantaneous detonation and instantaneous equilization of pressure during the expansion of the chamber

$$\rho/\rho_n = (r_0/R)^3;$$

at the shock-wave front in the medium (at the precursor)

$$p - p_0 = \rho_0 u D, \quad (\rho - \rho_0)D = \rho u$$

(r_0 is the radius of the explosive charge, D is the velocity of the shock-wave front).

We change over to dimensionless quantities and dimensionless Lagrange variables

$$p^0 = p/p_n, \quad p_0^0 = p_0/p_n, \quad \rho_0 = \rho/\rho_n, \quad V^0 = V/V_n',$$

$c^0 = c/c_n$, $u^0 = u/c_n$, $D^0 = D/c_n$, $R^0 = R/r_0$, $r^0 = r/r_0$, $t^0 = tc_n/r_0$, where $c_n = \sqrt{k_n p_n/\rho_n}$.

In the new variables the equations of dynamic (1.3) and static (1.4) compressibility have the form

$$\frac{V_D^0}{V_0^0} = \alpha_1 + \sum_{i=2}^{3}\alpha_i\left[\frac{\gamma_i(p^0 - p_0^0)}{k_n\rho_{i0}c_{i0}^{02}} + 1\right]^{-1/\gamma_i},$$

$$\frac{V_S^0}{V_0^0} = \sum_{i=1}^{2}\alpha_i\left[\frac{\gamma_i(p^0 - p_0^0)}{k_n\rho_{i0}c_{i0}^{02}} + 1\right]^{-1/\gamma_i},$$

TABLE 1

Media	α_1	α_2	α_3	A, kg/(sec·m²)	η, kg/(sec·m)
Water-saturated soils	0,01	0,39	0,6	$3{,}28\cdot10^6$	$1{,}09\cdot10^2$
Water	0,04	0,36	0,6	$3{,}39\cdot10^6$	$1{,}13\cdot10^2$
Gas	0,01	0,99	—	$1{,}49\cdot10^6$	$0{,}495\cdot10^2$

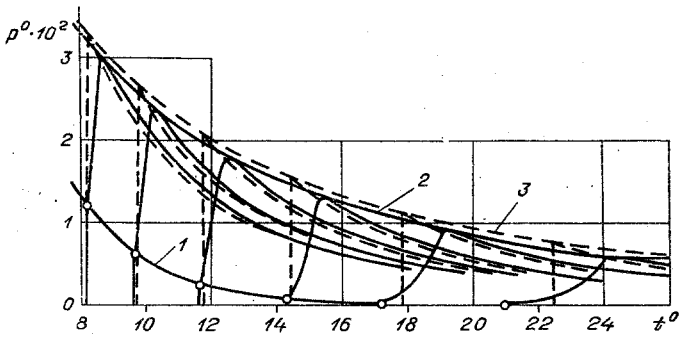

Fig. 3

and Eq. (1.2) determining the behavior of the medium becomes

$$\frac{\partial V^0}{\partial t^0} = -\frac{\partial p^0}{\partial t^0}\left(\frac{\rho_n}{\rho_0}\right)\frac{1}{k_n}\sum_{i=2}^{3}\frac{\alpha_i}{\rho_{i0}c_{i0}^2}\left[\frac{\gamma_i\left(p^0-p_0^0\right)}{k_n\rho_{i0}c_{i0}^2}+1\right]^{-\frac{1+\gamma_i}{\gamma_i}} -$$

$$-\frac{\alpha_1 r_0}{\eta}\left(\frac{\rho_n}{\rho_0}\right)\frac{p_n}{c_n}\left[p^0-\rho_0^0\alpha_1^{\gamma_1}\left\{\frac{V^0}{V_0^0}-\sum_{i=2}^{3}\alpha_i\left[\frac{\gamma_i\left(p^0-p_0^0\right)}{k_n\rho_{i0}c_{i0}^2}+1\right]^{-\frac{1}{\gamma_i}}\right\}^{-\gamma_1}\right]. \qquad (1.9)$$

In contrast to (1.2), Eq. (1.9) contains the ratio r_0/η and not $1/\eta$. The viscosity coefficient η is found experimentally. According to [1] the approximate values of η are given by the formula

$$\eta = Ar_*/3, \qquad (1.10)$$

where A is the acoustic resistance (impedance) of the two-component medium (solid and liquid particles) surrounding the gas bubbles,

$$A=\left(\frac{\alpha_2\rho_{20}+\alpha_3\rho_{30}}{1-\alpha_1}\right)^{1/2}\left(\frac{\alpha_2}{\rho_{20}c_{20}^2}+\frac{\alpha_3}{\rho_{30}c_{30}^2}\right)^{-1/2},\quad \frac{r_0}{\eta}=\frac{Ar_0}{3r_*},$$

and r_* is the radius of the gas bubbles (all bubbles of the same radius). In the water–air medium we get

$$A=\rho_{20}c_{20}/\alpha_2^{1/2}.$$

It follows from (1.10) that the ratio r_0/r_* occurs in (1.9); i.e., in the new variables the solution is valid for all media where r_0/r_* has a given value.

The problem was solved for a trotyl-type explosive in water-saturated soil with $\alpha_1=0.01$, $\alpha_2=0.39$, and $\alpha_3=0.6$, and values of $r_0/r_*=0.01$, 0.02, and 0.002. In the computations we took $k_n=3$, $k_0=1.25$, $p_n=96{,}000\cdot10^5$ N/m², $\rho_n=1600$ kg/m³, $Q=1000$ cal/g, $c_n=4250$ m/sec, $\rho_{10}=1.20$ kg/m³, $\rho_{20}=1000$ kg/m³, $\rho_{30}=2650$ kg/m³, $c_{10}=330$ m/sec, $c_{20}=1500$ m/sec, $c_{30}=4500$ m/sec, $\gamma_1=1.4$, $\gamma_2=7$, $\gamma_3=4$.

The values of A and η for some media are given in Table 1. The values of η correspond to $r_*=0.01$ cm.

The solution was obtained by the method of characteristics using a computer; the use of this method for media with volumetric viscosity was discussed in [1, 2]. A continuous computation of the spherical problem in a viscous medium from the instant of explosion to the time when the wavefront (precursor) reaches distances of the order of $100r_0$ is difficult, since it requires a large amount of computer time. This is due to the nature of the wave profile. At large distances from the explosion it contains segments of very slow and very rapid pressure increase (the transition zone ahead of the pressure maximum). For the computation of the transition zone 10-20 points are needed. For the uniform grid this requires the introduction of 10,000

points. Therefore, a simplified variant of the solution was chosen. The wave was computed successively in the following regions: $1 \leq r^0 \leq 2.5$; $2 \leq r^0 \leq 6$; $5 \leq r^0 \leq 17$; $15 \leq r^0 \leq 30$; $r^0 \geq 30$.

In the section $r^0 = 1$ the pressure was specified in the form $p^0 = p^0(R^0)$; at the subsequent positions it was specified in the form $p^0(t^0)$ taking into consideration the solution in the preceding region. Overlapping regions confirmed the accuracy of the solution.

§ 2. We now discuss the results of computations of the wave in the viscous medium with $r_*/r_0 = 0.01$ and in a nonviscous medium. Curves 1-3 in Fig. 1 show, respectively, the pressure at the wavefront (precursor), the maximum pressure, and the pressure at the boundary of the gas chamber as a function of the distance in the viscous medium. Curve 4 corresponds to the maximum pressure in the nonviscous medium. The pressure distribution $p^0(r^0)$ in these media is also shown for five time instants. Here and below the solid curves refer to the viscous medium and the dashed curves to the nonviscous medium. The maximum pressure in the viscous medium is smaller than in the nonviscous medium by 5-7%. In both media the pressure at the investigated distances increases discontinuously; however, the jump is smaller in the viscous medium. At $r^0 = 2$ the magnitude of the pressure jump in the viscous medium is about 0.75 of its value in the nonviscous medium. In the viscous medium the pressure behind the jump increases to the maximum continuously.

The change in the state of the particles of the medium during the passage of the wave at distances $r^0 = 1$, 1.1, 1.3, 1.7, 2.8 is shown in Fig. 2a. Curves 1, 2 correspond to the diagrams of dynamic and static compression of the medium. It is evident that after the shock compression at the precursor OF, occurring according to the dynamic diagram, the state is close to the static diagram along the lines FM, which are a continuation of the straight line OF for all points except the first. The discharge occurs practically according to the static diagram. At these distances the minimum volume in the viscous medium is obtained at the maximum pressure. A similar nature of the change of state is retained at moderate pressures (see Fig. 2b). At relatively small pressures (see Fig. 2c) the lines FM are not rectilinear, the minimum volume is obtained during the period of pressure decrease, and the discharge of the medium occurs along the curve lying beyond the diagram of static compression.

The time dependence of the pressure $p^0(t^0)$ in particles with $r^0 = 5.7$, 6.3, 7.1, 8.1, 9.3, 10.7 in viscous and nonviscous media is shown in Fig. 3. In the viscous medium the precursor moves on and the magnitude of the jump rapidly decreases to zero (denoted by circles). Curve 1 gives the pressure change at the precursor, curve 2 gives the maximum pressure in the viscous medium, and curve 3 gives the maximum pressure in the nonviscous medium. The difference between the maximum pressures in the viscous and nonviscous media does not exceed 8%. For $r^0 > 9$ the pressure at the precursor is practically equal to p_0^0; here the maximum dimensional pressure in the wave is $p \sim 800 \cdot 10^5$ N/m^2. The time taken for the pressure to reach its maximum increases with the distance of the wave from the point of explosion.

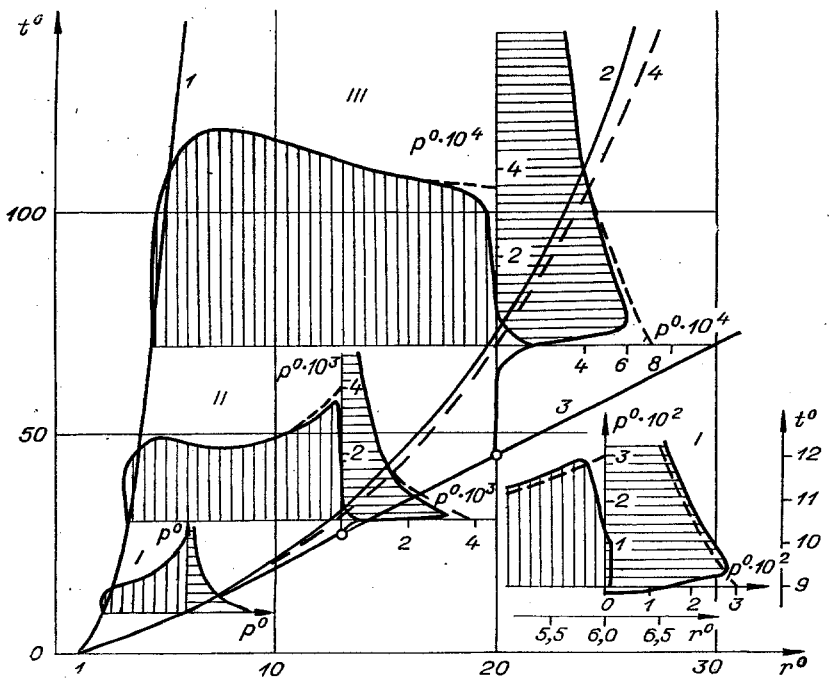

Fig. 4

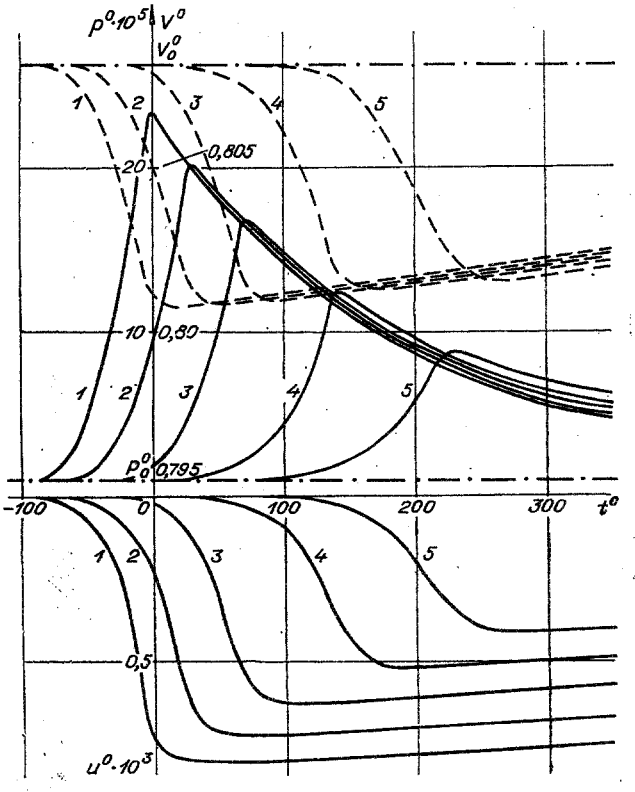

Fig. 5

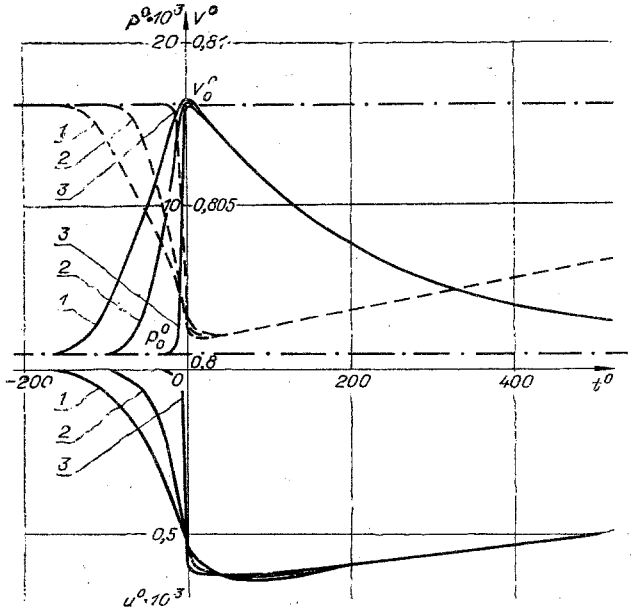

Fig. 6

The results of the computation of the pressure in the viscous (for $r_*/r_0 = 0.01$) and nonviscous media are shown in Fig. 4. Curves 1-3 give the trajectory of motion of the boundary of the gas chamber in the viscous medium, the pressure maximum, and the precursor, respectively; curve 4 corresponds to the pressure maximum in the nonviscous medium. The pressure maximum in the viscous medium moves with a velocity close to the velocity of the maximum in the nonviscous medium, i.e., the velocity determined by the static compression diagram; curves I-III correspond to the pressure distribution in the medium (vertical hatching) at time instants 9.5, 30, 70; the shock front in the nonviscous medium attains distances $r^0 = 6$, 13, 20. The graphs of the change of pressure with time $p^0(t^0)$ (horizontal hatching) are also plotted for the same distances. A part of the position of I is shown on enlarged scale in the right bottom corner.

The difference between the maximum pressures in the viscous and nonviscous media at all distances does not exceed 12%. The wave profiles $p^0(t^0)$ are significantly different. In the nonviscous medium the wave remains a shock wave; in the viscous medium the jump gets smeared. At a sufficient distance from the explosion point the pressure (after the arrival of the precursor) remains almost equal to zero for some time and only later begins to increase to its maximum value. The length τ_* of this transition zone of intense increase at a distance $r^0 = 20$ is smaller than one half the time τ from the arrival of the precursor to the arrival of the maximum pressure. As the separation from the explosion point increases, τ and τ_* increase, but τ_* increases appreciably more slowly. After the maximum is attained, the dependence $p^0(t^0)$ is practically identical in both media. Thus, noticeable differences in the wave profiles with and without the viscosity are observed mainly in the time period before the maximum pressure is obtained within the particle.

As in the case of the pressure, the differences between the extremal values of the volume and the velocity of the particles, computed with and without viscosity, do not exceed a few percent. The main difference of the functions $V^0(t^0)$ and $u^0(t^0)$ in these media is the presence of the jump in the absence of viscosity and the continuity of the change in the viscous medium. The extremal values of the particle velocity, the volume, and pressure in the viscous medium are attained almost simultaneously at these distances.

The graphs of $p^0(t^0)$, $u^0(t^0)$ (solid curves) and $V^0(t^0)$ (dashed curves) at distances $r^0 = 30, 32, 35, 40, 45$ in the viscous medium are shown in Fig. 5.

The graphs cover the region of increase of the parameters, in which their values are noticeably different from the initial values (for the pressure it is time τ^*), and the region of decrease. The time period immediately after the arrival of the precursor, when the parameters are practically equal to their initial values, is not included. The extremal values of the parameters decrease as the distance from the explosion increases and the time required to attain these extrema increases. At these distances the volume and the velocity of the particles attain their extrema not at the maximum pressure near the explosion, but during the period of the pressure decrease. The difference in the duration of the pressure increase, the velocity of the particles, and the volume increase with the distance from the explosion. The rate of decrease of the values of all three parameters decreases as the distance and the total duration of the wave increases.

We now discuss the results of investigation of the dependence of the wave parameters on the viscosity coefficient or equivalently on the radius of the bubble. For the viscous medium with $\alpha_1 = 0.01$ and $r_*/r_0 = 0.01$ the dependence $p^0(t^0)$ is obtained for $r^0 = 30$ and this is used to compute the wave parameters at large distances in the nonviscous and viscous media for $r_*/r_0 = 0.02$, 0.01, and 0.002.

The computations show that the maximum pressure can be approximated by the formula

$$p_m^0 = p_1^0 (r_1^0/r^0)^\beta, \; r^0 \geqslant r_1^0,$$

where $r_1^0 = 30$, $p_1^0 = 22.3 \cdot 10^{-5}$ (maximum pressure) at r_1^0. The quantity β in the nonviscous medium and the viscous medium with $r_*/r_0 = 0.02$, 0.01, and 0.002 comprises 2.55, 2.52, 2.43, and 2.37, respectively. The pressure decreases most intensely in the nonviscous medium. The intensity of the decrease in the viscous medium decreases with the increase in the radius of the bubble, i.e., with the increase of the viscosity coefficient η. The difference is small: At a distance $r^0 = 50$ in the nonviscous medium and in the viscous medium with $r_*/r_0 = 0.02$ it is less than 5%.

Thus, at small distances from the explosion the maximum pressure decreases more intensely in the viscous medium, while at large distances it decreases more intensely in the nonviscous medium. A similar feature was noted earlier in the case of plane waves [3].

The dependences $p^0(t^0)$, $u^0(t^0)$ (solid curves) and $V^0(t^0)$ (dashed curves) in the viscous medium at a distance $r^0 = 35$ are shown in Fig. 6 for different radii of the bubble. Curves 1-3 pertain to the values $r_*/r_0 = 0.02$, 0.01, and 0.002, respectively. In the segment $\Delta r^0 = 5$ the maximum pressure changes insignificantly (by 1-2%) on increasing the bubble radius by an order of magnitude. The wave profile changes significantly; the length of the transition zone of intense increase of the parameters increases by a factor of 5-7. The volume and the velocity of the particles attain their extremal values during the period of pressure decrease. The lag increases with the bubble radius. The nature of the decay of the parameters after the extremum is reached remains practically unchanged on changing the bubble radius by an order of magnitude. The increase of the viscosity coefficient leads to an increase of the intensity of wave smearing.

Let us compare the values of the wave parameters in the viscous medium and the nonviscous medium but computed according to the dynamic diagram of the viscous medium. The values of p^0, D^0, and u^0 computed for

TABLE 2

r^0 \ α_1	p^0		D^0		u^0	
	0	0,01	0	0,01	0	0,01
5	$0{,}52\cdot10^{-1}$	$0{,}43\cdot10^{-1}$	0,502	0,452	$0{,}27\cdot10^{-1}$	$0{,}26\cdot10^{-1}$
10	$0{,}17\cdot10^{-1}$	$0{,}93\cdot10^{-2}$	0,434	0,323	$0{,}1\cdot10^{-1}$	$0{,}77\cdot10^{-2}$
20	$0{,}66\cdot10^{-2}$	$0{,}68\cdot10^{-3}$	0,407	0,131	$0{,}43\cdot10^{-2}$	$0{,}14\cdot10^{-2}$
30	$0{,}40\cdot10^{-2}$	$0{,}24\cdot10^{-3}$	0,400	0,080	$0{,}26\cdot10^{-2}$	$0{,}75\cdot10^{-3}$
40	$0{,}28\cdot10^{-2}$	$0{,}13\cdot10^{-3}$	0,396	0,057	$0{,}19\cdot10^{-2}$	$0{,}48\cdot10^{-3}$
50	$0{,}21\cdot10^{-2}$	$0{,}9\cdot10^{-4}$	0,394	0,046	$0{,}15\cdot10^{-2}$	$0{,}36\cdot10^{-3}$

$\alpha_1 = 0$ and 0.01 according to the model without viscosity are shown in Table 2. In the first case the compression diagram practically coincides with the dynamic diagram of the viscous medium; in the second case it coincides with the static diagram. As mentioned above, the results of the computation according to the static diagram differ from those for the viscous medium only by a few percent. Table 2 shows that even at $r^0 = 20$ in the viscous medium the maximum pressure is an order of magnitude smaller than in the computations according to the dynamic diagram; the particle velocity and the velocity of the maximum D^0 differ by a factor of 3. Subsequently the difference increases. Thus, the wave parameters in the viscous medium are significantly different from the parameters computed according to the dynamic diagram.

§ 3. The experiments show that in soils there exists a similarity for detonation waves; on the other hand, in a medium having volumetric viscosity the similarity need not necessarily be there. The computations carried out here enable us to explain this apparent contradiction. Let the radius of the gas bubbles in a medium with $\alpha_1 = 0.01$ be equal to 0.05 cm. Then curve 1 in Fig. 6 pertains to an explosive charge of radius $r_0 = 2.5$ cm and curve 3 to $r_0 = 25$ cm. On changing the radius by an order of magnitude, i.e., on changing the mass of the charge by three orders of magnitude, the extremal values of the pressure, particle velocity, and detonation-wave velocity change at similar distances only by a few percent. Considering the intrinsic scatter of the properties of the soil (for example, content α_1) it is not possible to perceive such a difference in the experiments. The similarity principle is not exactly satisfied; however, the deviations of the extremal values of the wave parameters from the similarity are small and cannot be verified experimentally. Computations show that the time for the increase of the wave parameters to the extrema depends substantially on the scale of the phenomenon. With the increase of the charge mass by three orders of magnitude the growth time at a distance $r^0 = 35$ increases by a factor of 5-7. This result can be verified experimentally. The lag of the minimum volume in relation to the pressure maximum also increases with the increase of the mass of the charge.

The problem of propagation of a spherical detonation wave in a nonviscous medium is solved in [9] based on the model of [6]. The computations are done for five water-saturated soils with the content of the gaseous component varying from 0 to 0.04. It is shown that the wave parameters have a significant dependence on α_1. At sufficient distances from the explosion point with the increase of α_1 in this range the maximum pressure decreases by two orders of magnitude and the velocity of propagation of the maximum pressure and the particle velocity decrease by an order of magnitude. A comparison of the computational results with those of the experiments conducted on water-saturated soils in field conditions for the mass of the explosive charge varying from 1 to 100 kg shows a good agreement.

At the same time the computations showed that the wave is a shock wave at all distances for all α_1. In the experiments for $\alpha_1 = 0$ the wave is actually a shock wave but for $\alpha_1 > 0$ smearing is observed. The time of the increase of the pressure to the maximum increases with α_1 and for $\alpha_1 = 0.04$ it reaches tens of milliseconds. Computations done on the basis of the model of the multicomponent medium with volumetric viscosity show that it reflects the properties of real media more accurately and completely than the model without viscosity. The extremal values of the parameters depend substantially on the content of the gaseous component and their dependence on the viscosity coefficient η is considerably weaker. An order of magnitude change in η changes their values by a few percents. The smearing of the detonation wave and its transformation from a shock wave to a continuous compression wave depend substantially on both α_1 and η. The intensity of smearing increases with the increase in α_1 and η. Away from the explosion the extremal values of the particle velocity and volume are attained during the period of pressure decrease. The extremal values of the parameters can be computed approximately from the model without viscosity according to the static diagram of the model of the viscous medium; for determining the temporal characteristics, i.e., the time for reaching these values, and the wave profiles $p^0(t^0)$, $u^0(t^0)$, and $V^0(t^0)$ it is necessary to use the model of a medium with volumetric viscosity.

The authors express gratitude to L. I. Sedov and S. S. Grigoryan for discussion of the work.

LITERATURE CITED

1. G. M. Lyakhov, Fundamentals of Dynamics of Detonation Waves in Soils and Rocks [in Russian], Nedra, Moscow (1974).
2. G. M. Lyakhov and V. N. Okhitin, "Plane waves in nonlinear, viscous, multicomponent media," Zh. Prikl. Mekh. Tekh. Fiz., No. 2 (1977).
3. G. M. Lyakhov and V. N. Okhitin, "Plane nonstationary waves in media with volumetric viscosity," Zh. Prikl. Mekh. Tekh. Fiz., No. 5 (1977).
4. S. S. Grigoryan, "Basic concepts of soil dynamics," Prikl. Mat. Mekh., 24, No. 2 (1960).
5. É. A. Koshelev, "Development of camouflet cavity during explosion in a soft soil," Zh. Prikl. Mekh. Tekh. Fiz., No. 2 (1975).
6. G. M. Lyakhov, "Shock waves in multicomponent media," Izv. Akad. Nauk SSSR, Mekh. Mashinostr., No. 1 (1959).
7. Z. Legowski and E. Wlodarczyk, "Regular reflection of an oblique stationary shock wave from an indeformable plane partition in saturated soil," Proc. Vibr. Probl., Pol. Acad. Sci., 15, No. 2 (1974).
8. F. Chwalczyk and E. Wlodarczyk, "O pewnei metodzie konstrukcji rozwiazania problemu propagacju plaskiej niestacjonarnej fali underzeniowej w osrodkax niesprezistych," Biul. Woisk. Akad. Techn., No. 4 (1971).
9. G. M. Lyakhov, Fundamentals of Dynamics of Detonation Waves in Soils and Rocks [in Russian], Nedra, Moscow (1974).
10. Kh. A. Rakhmatulin, "Wave propagation in multicomponent media," Prikl. Mat. Mekh., 33, No. 4 (1969).
11. S. K. Godunov and N. S. Kozin, "Structure of shock waves in a viscoelastic medium," Zh. Prikl. Mekh. Tekh. Fiz., No. 5 (1974).
12. L. V. Kashpriskii, L. P. Orlenko, and V. N. Okhitin, "Effect of equation of state on the dispersion of detonation products," Zh. Prikl. Mekh. Tekh. Fiz., No. 2 (1973).

OPTIMUM CONDITIONS FOR EXCITATION OF ELASTIC VIBRATIONS IN SOLIDS BY PULSED IONIZING RADIATION

V. D. Volovik and S. I. Ivanov

UDC 534.231+539.121.7

Investigations of elastic vibrations accompanying the interaction of pulsed ionizing radiation with solids have shown that mechanical stresses are produced by an unsteady thermoelastic body force $\mathbf{F}(\mathbf{r}, t)$ [1, 2]

$$\mathbf{F}(\mathbf{r}, t) = -\Gamma \nabla E(\mathbf{r}, t), \tag{1}$$

where Γ is the Grüneisen constant of the target material and $E(\mathbf{r}, t)$ is the energy absorbed from the beam of ionizing radiation per unit volume of target material.

Ordinarily nonstationary thermoelasticity problems require the simultaneous solution of the wave equation and the heat-conduction equation. If the duration of a pulse of charged particles τ_0 interacting with a solid target satisfies the condition

$$\tau_{ei} \ll \tau b \ll \tau_T \simeq r_b^2/\varkappa, \tag{2}$$

the propagation of heat does not have to be taken into account during a time on the order of magnitude of the pulse duration. Here τ_{ei} is the time to establish uniform temperature conditions in the electron and ion subsystems of the material, τ_T is the characteristic time for heat to diffuse from the region heated by a beam of radius r_0, and $\varkappa$ is the thermal diffusivity of the target material.

If condition (2) holds, and in addition $\tau_S = r_b/s \ll \tau_T$, the temperature of the region heated by the beam can be considered constant even for a time τ_S – the time for an acoustic wave propagating with velocity s to leave this region. In this case the problem of finding the displacement of elastic waves $\mathbf{u}$ excited by a pulsed beam of particles is reduced to the problem of solving the wave equation, which for an infinite target can be written in the form

Khar'kov. Translated from Zhurnal Prikladnoi Mekhaniki i Tekhnicheskoi Fiziki, No. 6, pp. 137-140, November-December, 1977. Original article submitted November 23, 1976.

 0021-8944/77/1806-0842$07.50